A Computational Technique for Heat Transfer Due to a Fast Moving Heat Source

K.V. Rama Rao and J.A. Sekhar

Defence Metallurgical Research Laboratory, Hyderabad-500 258

ABSTRACT

The heat transfer in the two phase region in the study of melting and solidification of a surface layer by a moving heat source is studied. The transient problem is formulated using the enthalpy and temperature model and solved in an oblate spheroidal co-ordinate system using an implicit modified upwinding scheme in terms of non-dimensional nodal enthalpy and temperature. It is observed that the temperature gradient which controls the solidification rate, increases to a maximum initially and then decreases to zero. It is found that the solid-liquid interface velocity which is zero initially very quickly reaches to the velocity of the heat source, though the gradient ahead of the interface relaxes much more slowly.

NOMENCLATURE

a	radius of the circular region (m) of the top hat beam profile
	specific heat, $Jkg^{-1}K^{-1}$
f_L	fraction liquid in any discretized volume in the finite difference scheme
F_0	Fourier number ($kT/\rho C_p a^2$)
G_L	non-dimensional temperature gradient in the liquid at the solid-liquid interface
	temperature gradient in the liquid at any position ahead of solid/liquid interface (K/m)
h	scale factor
H	specific enthalpy, JKg^{-1}
∇H_{sl}	heat of fusion, JKg^{-1}

k thermal conductivity $Jm^{-1}s^{-1}K^{-1}$

P rate of heat generation per unit volume, Wm^{-3}

q absorbed heat flux, Wm^{-2}

t time, s

T temperature, K

T^* non-dimensional temperature $(k(T-T_0 + \nabla H_{sl}/C_p)\, U/2aq)$

T_0 ambient temperature, K

T_M melting temperature, K

u_1, u_2, u_3 oblate spheroidal co-ordinates

U velocity of heat source, ms^{-1}

V' velocity of solid-liquid interface. ($V' = U$ at steady state with respect to an observer fixed to the solid

V volume, m^3

v velocity, ms^{-1}

V^* velocity of solid-liquid interface for an observer fixed to the heat source ($V^* = 0$ at steady state)

x_w half width of resolidified trail on the xy plane

x, y, z Cartesian co-ordinates

a thermal diffusivity $(k/\rho C_p)$, $m^2 s^{-1}$

Θ dimensionless temperature

ψ dimensionless enthalpy variable

ρ density, kgm^{-3}

j, k, m nodal point subscripts in u_1, u_2, u_3 and t directions respectively

1. INTRODUCTION

Understanding of the solid-liquid phase change heat transfer phenomena is gaining impetus because of its applications in many naturally occurring and engineering processes such as tne formation of ice on a lake, the freezing of water pipes, freezing of food-stuffs, thermal control of spacecraft, processes in thermal energy storage systems and metal processing.

Modelling of these problems is complicated by the fact that more than one phase exists simultaneously and the interface, a region of discontinuity separating these two phases, moves with time. As the physical variables such as thermal conductivity, density etc., are different in the two phases, the problem is to be solved separately in each phase and the solutions matched at the interface taking into account the jump conditions.

The availability of high intensity-sources such as electron beams and various types of lasers has led to the development of a number of new material processing techniques. In the present investigation we have considered once such application, namely, the rapid surface melting and solidification by a fast moving heat source. Several recent

publications[1-17] have dealt with the heat flow characteristics during the passage of, or the stationary switching of a heat source and these have been verified by experiments. However, all these investigations have been confined to quasi-steady continuous moving beams[9-13]. In a recent paper[18], we have examined both the initial transient and the final quasi-steady state. The computational technique used there is an extension of the one used in ref. 3 and is valid only for small beam velocities. We have presented a new computational technique based an upwinding scheme for higher beam velocities.

2. MATHEMATICAL FORMULATION

Let us consider a beam such as an electron beam or a laser beam of high intensity over a circular region of a semi-infinite solid moving with a velocity U. This situation is shown schematically in Fig. 1. The surface layer absorbs heat and melts. Temperature profiles, the solid-liquid interface and other parameters are to be calculated. The co-ordinate system is located at the centre of the beam and is moving with it. The heat conduction equation in temperature and enthalpy formulation in generalised co-ordinates[3] is written as

$$\frac{\delta}{\delta u_1}\left(\frac{k_1 h}{h_1^2}\frac{\delta T}{\delta u_1}\right) + \frac{\delta}{\delta u_2}\left(\frac{k_2 h}{h_2^2}\frac{\delta T}{\delta u_2}\right) + \frac{\delta}{\delta u_3}\left(\frac{k_3 h}{h_3^2}\frac{\delta T}{\delta u_3}\right) + \rho h =$$

$$\rho\frac{\delta}{\delta t}(hH) - \rho\left[\frac{hv_1}{h_1}\frac{\delta H}{\delta u_1} + \frac{hv_2}{h_2}\frac{\delta H}{\delta u_2} + \frac{hv_3}{\_\_\_}\frac{\delta H}{\_\_\_}\right] \tag{1}$$
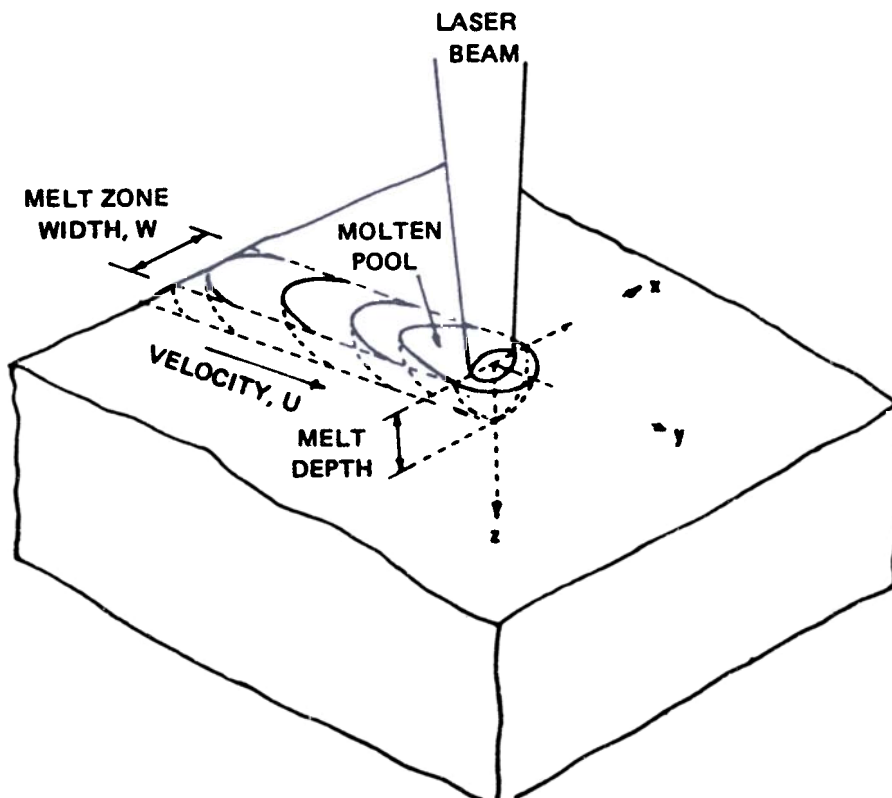

Figure 1. Schematic of a high heat intensity source (such as a laser beam) moving at a constant velocity U on a substrate. The axes of a co-ordinate system moving with the beam have been labelled.

where h_1, h_2, h_3 are scale factors in the three co-ordinate directions u_1, u_2, u_3 and v_1, v_2 and v_3 are the velocity components in the three directions respectively. k_1, k_2 and k_3 are the thermal conductivities in the three co-ordinate directions. T and H are the temperature and enthalpy and finally P is the source term accounting for the heat transferred by the beam. These equations are to be solved with the specified boundary condition to obtain the temperature distribution and other physical variables.

3. COMPUTATIONAL PROCEDURE

Before defining the finite-difference approximation in terms of upwind difference scheme, let us define the feed-back sensitivity. To do so, let us say, the finite-difference approximation of Eqn. (1) is given by :

$$\frac{\delta T_i}{\delta t} = RHS$$

where *RHS* contains terms independent of time and involves terms like T_i, T_{i+1}, T_{i-1} etc. To study the evolution of perturbations in T_i, we have to consider the variation of the above equation with T_i, i.e.,

$$\frac{\delta \delta T_i}{\delta t} = \frac{\delta RHS}{\delta T_i} \delta T_i$$

which has a solution of the form

$$\delta T_i = \exp |\int \Sigma dt |$$

where $\Sigma = \dfrac{\delta RHS}{\delta T_i}$ which is defined as the feed-back sensitivity

It is easy to see from this expression that a positive feed-back sensitivity leads to exponential growth of the perturbations and therefore is not desirable. On the other hand a negative feed-back sensitivity damps the perturbations and the algorithm is stable. In the case of a stationary beam (pure diffusion equation), the central difference approximation gives the feed-back sensitivity as

$$\Sigma = -2 \, \Gamma / \Delta x^2$$

where Γ is the thermal diffusivity (> 0).

Hence $\Sigma < 0$ always and as such, the scheme is stable. However, if the convective term is present, then for the convective part $\Sigma = 0$. Hence the negative feed-back sensitivity is entirely dependent on the diffusion term. Under convection dominant conditions this is very weak and the solution is susceptible to both temparol and spatial oscillations. However, when the convection term is approximated using first order upwinding scheme as

$$-u \frac{\delta T}{\delta x} = -u \frac{(T_{i+1} - T_{i-1})}{2\Delta x} + |u| \frac{(T_{i+1} - 2T_i + T_{i-1})}{2\Delta x}$$

the feed-back sensitivity is given by

$$\Sigma = - |u| / \Delta x$$

which is always negative and as such we have a stable scheme. However, this approximation introduces an artificial diffusion term given by $|u| / \Delta x/2$, which may corrupt the effect of the physical diffusion term unless it is made less than the physical diffusion term. To achieve this, we have modified the approximation as

$$-u\frac{\delta T}{\delta x} = -u\frac{(T_{i+1} - T_{i-1})}{2\Delta x} + |u|\beta\frac{(T_{i+1} - 2T_i + T_{i-1})}{2\Delta x} \tag{2}$$

where $\beta > 0$ and $\beta \ll 1$. Thus, we have suppressed the effect of artificial diffusion and at the same time have a positive feed-back sensitivity.

Before we write the finite-difference equations let us transform the co-ordinate system to oblate spheroidal as the metal pool formed during the process of heating has this shape. The transformation from cartesian co-ordinate system (x, y, z) to this system (η, ξ, ϕ) is given by

$$x = a \cosh \eta \sin \xi \cos \phi$$

$$y = a \cosh \eta \sin \xi \sin \phi$$

$$z = a \sinh \eta \cos \xi$$

The scale factor and velocity component are determined and a detailed description is given in ref. 18. Now using central difference approximation for space variable, viz., η, ξ, ϕ and forward difference for time and the modified upwinding scheme for the convective terms, the finite-difference approximation of Eqn. (1) is written as

$$C_s T^m_{i,j,k} = -\frac{D_1}{C_p} H^m_{i,j,k} \quad \frac{D_s}{C_p} H^m_{i,j,k} + C_1 T^m_{i-1,j,k} + C_2 T^m_{i+1,j,k}$$

$$+ C_3 T^m_{i,j-1,k} + C_4 T^m_{i,j+1,k} + C_5 T^m_{i,j,k-1} + C_6 T^m_{i,j,k+1}$$

$$\frac{C_7}{C_p} H^m_{i-1,j,k} + \frac{C_8}{C_p} H^m_{i+1,j,k} \quad \frac{C_9}{C_p} H^m_{i,j-1,k} + \frac{C_{10}}{C_p} H^m_{i,j+1,k}$$

$$\frac{C_{11}}{C_p} H^m_{i,j,k-} + \frac{C_{12}}{C_p} H^m_{i,j,k+1} - D_1 H^{m-1}_{i,j,k}$$

$$+ P a^2 (\cosh^2 \eta_i - \sin^2 \xi_j)/k_1$$

where i, j, k and *m* are the nodal indices in these co-ordinate directions and the time directions respectively,
and

$$(\Delta\eta)^{-2} \mp (2\Delta\eta)^{-2} \tanh \eta_i$$

$$k_2 k_1^{-1}(\Delta\xi)^{-2} \mp (2\Delta\xi)^{-1} \coth \xi_j$$

$$= \frac{(\cosh^2 \eta_i - \sin^2 \xi_j) \, k_3 \, k_1^{-1}(\Delta\phi)^{-2}}{\cosh^2 \eta_i \sin^2 \xi_j}$$

$$\frac{\rho U a C_p (L_1 \mp \beta |L_1|)}{2k_1 \Delta \eta_i}$$

$$= \frac{\rho U a C_p (L_3 \mp \beta |L_3|)}{2k_1 \Delta \xi_j}$$

$$C_{11,12} = \frac{\rho U a C_p (L_2 \mp \beta |L_2|)}{\cdot 2k_1 \Delta \phi_k}$$

$$L_1 = \sinh \eta_i \cosh \xi_j \sin \phi_k$$

$$L_2 \quad \sinh \eta_i \sinh \xi_j \sin \phi_j$$

$$L_3 = \frac{(\cosh^2 \eta_i - \sin^2 \xi_j)}{\cosh \eta_i \sin \xi_j} \cos \phi_k$$

The dimensional nodal enthalpy and the temperature are now defined as

$$\frac{1}{\rho V} \int_V \frac{\rho(H - H_{SL}^*)}{\Delta H_{SL}} = \frac{H - H_{SL}^*}{\Delta H_{SL}}$$

$$\frac{C_p(T - T_M)}{\Delta H_{SL}}$$

and satisfy the following relations.

In the solid phase

$$\psi = \Theta \quad \frac{C_p(T - T_M)}{\Delta H_{SL}}$$

and in the superheated region

$$\psi = \Theta + 1 = \frac{C_p(T - T_M)}{\Delta H_{SL}} + 1 >$$

and in the interface

$$0 \leqslant \psi \leqslant 1.0 \text{ and } \Theta = 0$$

finally

$$P_{i,j,k}^m = \frac{q\, a \cos \xi_j \sin \Delta \xi}{\cosh \eta_i (\cosh^2 \eta_i - \sin^2 \xi_j)} \quad \frac{1}{\Delta \xi \Delta \eta}$$

In terms of the new variable, the equation now assumes the final form as

$$(C_s + D_s + D_l)\, \psi_{i,j,k}^m = f\left(\Theta_{i,j,k}^m, \psi_{i,j,k}^{m-i}\right)$$

4. BOUNDARY CONDITIONS

A complete discussion on the boundary conditions is given by Hsu, et al.[3], and the boundary conditions are given by

a) $\eta = 0 \le \zeta \le \pi/2, -\pi/2 < \phi < \pi/2, \delta T/\delta\eta = 0$

and consequently $C_1 = C_7 = 0$

b) $\eta > 0, 0 \le \zeta \le \pi/2, \phi = -\pi/2, \delta T/\delta\phi = 0, P = 0$

resulting $C_5 = C_{11} = 0$

c) $\eta > 0, 0 \le \zeta < \pi/2, \phi = \pi/2 \; \delta T/\delta\phi = 0, P = 0$

so that $C_6 = C_{12} = 0$

d) $\eta \to \infty \; 0 \le \zeta < \pi/2, -\pi/2 < \phi < \pi/2 \; P = 0$

resulting $C_3 = C_9 = 0$

e) $\eta > 0 \; \zeta = \pi/2, -\pi/2 < \phi < \pi/2 \; P = 0$

so that $C_4 = C_{10} = 0$

The system of equations along with the boundary conditions are solved as follows : initially at time $t = 0$, the non-dimensional temperature ψ is given, using which the value of ψ at the next time level is calculated using a point iterative method such as Gauss-Seidel method. The convergence criteria used for the iteration is

$$|\psi^m_{i,j,k} \text{ (new)} - \psi^m_{i,j,k} \text{ (old)}| < 10^{-4}$$

Once the value of ψ is calculated to the desired accuracy, the value of Θ is obtained using the relations (3). This cycle is repeated for all points of the substrate. Now using the values of ψ and Θ at the mth time level, new values of the variables are calculated at $(m+1)^{th}$ time level exactly the same way until a steady state is reached. Here the satisfying condition is taken as

$$|\psi^{m+1}_{i,j,k} - \psi^m_{i,j,k}| < 10^{-4}$$

Calculations were carried out for a number of parameters and some salient features of the problem are discussed in the next section.

5. DISCUSSION OF RESULTS

The temperature distribution along the y axis of the substrate for various values of the non-dimensional velocity $Ua/2a$ is presented in Fig. 2. One important observation obtained from the figure is that the slope (temperature gradient) increases to a maximum value at $y/a = 1$ and then starts decreasing to a value zero which implies that the maximum cooling rate during solidification occurs at $r/a = 1$. In Fig. 3 we have presented the dimensionless temperature gradient for a typical velocity $Ua/2a = 0.9$, from which it is seen that the gradient reaches a maximum at $r/a = 1$. There is a more interesting peak at the interface and it is necessiated by the requirement of a concave profile at the interface. A concave temperature gradient in the liquid increases as the solid-liquid interface is approached from the centre of the beam. The development of the temperature $T(0, 0, 0)$ to a steady state is represented in Fig. 4 and it is seen that it takes a dimensional time $F_0 = 10$ to reach steady state. The interface position along the x,z and y axis (Fig. 5) takes dimensional values of 10, 10 and 20 respectively to reach steady state. At a velocity of 0.1 m/s and a beam radius of 5×10^{-4} m for an aluminium substrate a distance of 45 mm is covered in a dimensional time of $F_0 = 20$, before steady state is achieved. We have presented the
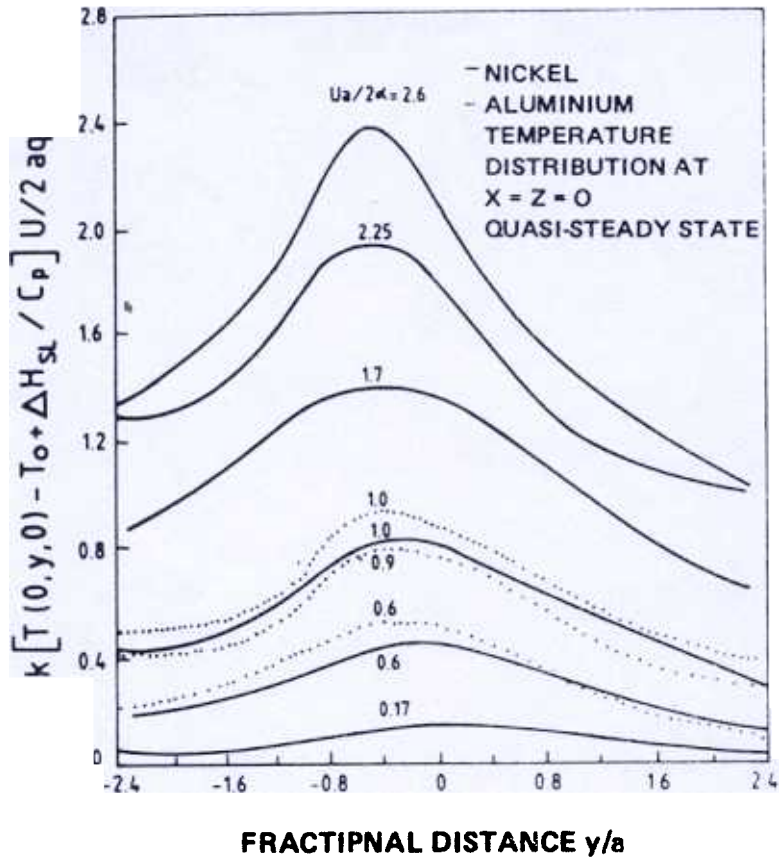
Figure 2. Quasi-steady state dimensionless temperature distribution along the *y*-axis of the moving heat flux showing trends for different substrate materials.
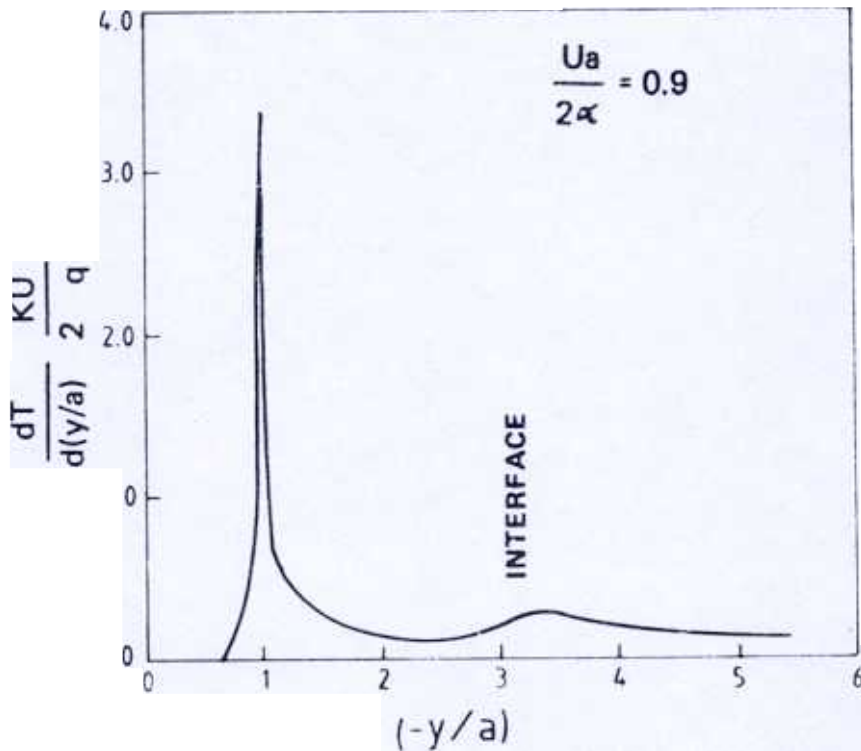

Figure 3. Dimensionless temperature gradient along the $(-y/a)$ direction at $z = 0$. The respective values of *qa* and $Ua/2\alpha$ are 6.4×10^5 W/m and 0.9.
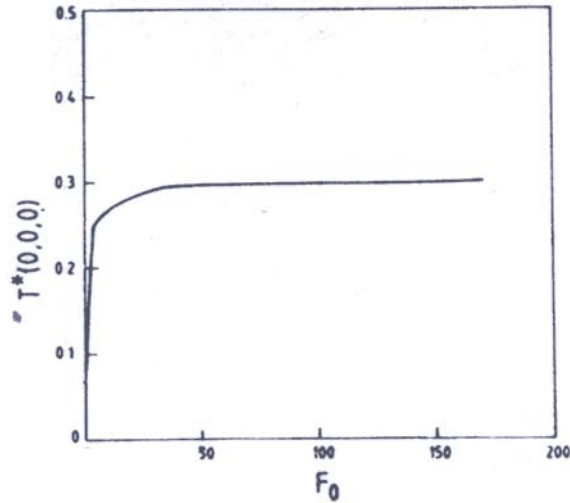
Figure 4. Dimensionless temperature $T^*(0,0,0)$ as a function of dimensionless time F_0. The qa and $Ua/2a$ values respectively are 6.4×10^5 W/m and 0.3.
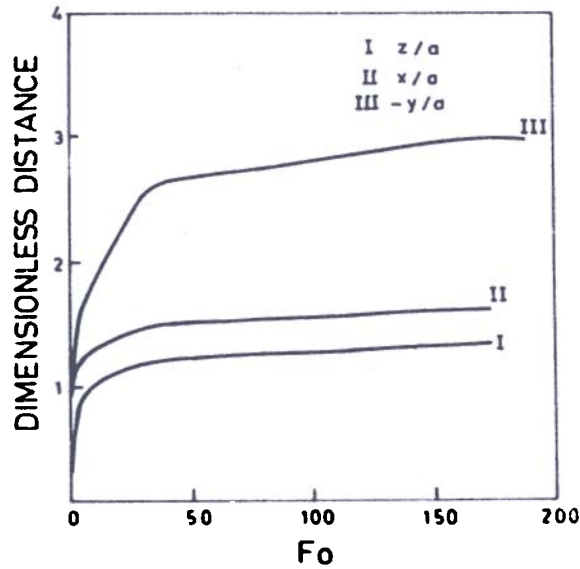

Figure 5. Dimensionless interface position along the x, y, and z axis as a function of dimensionless time F_0. The values of qa and $Ua/2a$ are 6.4×10^5 W/m and 0.3.

Table 1. Direction of change in the depth and width of the steady state melt with increase in material constants

Material constants	k	$\dfrac{\Delta H_{sl}}{C_p}$	T_0	T_m
Melt depth or width			↑	

↑ = Increases

↓ = Decreases

Table 2. Solidification parameters during the initial transient

F_0	Time (s)	G_L^* (km^{-1})	Peak G_L^* (km^{-1})	V^* (ms^{-1})	$V = (U+V)$ (ms^{-1})
0.335					0.07
		1.29×10^6	2.7×10^6		0.1
	10^{-1}	5×10^5	2.6×10^6	-5×10^{-6}	0.1
167.5	0.5	3.5×10^5	2.7×10^6	0	0.1

$qa = 6.4 \times 10^5$ W/m $U = 0.1$ m/s

dimensional temperature for various non-dimensional times. It is to be noted that this curve is similar to the one shown in Fig. 2. The inflexion in the temperature gradient is observed even for low Fourier numbers. Finally in Table 2, we have the temperature gradient (G_L^*) and peak (G_L^*) and the interface velocity V for various times. Initially the solid-liquid interface velocity is zero and very quickly achieves the beam velocity. However the gradient a head of the interface relaxes much more slowly. Experimental verification of these results was carried out by using a multi mode 5kW CO_2 laser and the details are presented elsewhere[18]. We have also established theoretically[19] using pulsed lasers that the cooling rates can be controlled and so is surface solidification.

ACKNOWLEDGEMENTS

REFERENCES

1. Rosenthal, D., *Welding Journal*, **20** (1941), 2205.

2. Carslaw, H.S. & Jaeger, J.C., (Eds), Conduction of Heat in Solids, (Oxford University Press), 1978, p. 270.

3. Hsu, S.C., Kou, S. & Mehrabian, R., *Metall. Trans.*, **118B** (1980), 30.

4. Cohen, M.I., *J. Franklin Inst.*, **283** (1967), 271.

5. Kou, S., Hsu, S.C. & Mehrabian, R., *Metall. Trans.*, **12B** (1981), 33.

6. Cline, H.E. & Anthony, T.R., *J. Appl. Phy.*, **48** (1977), 4906.

7. Nissim, H.I., Litoila, A., Good, R.B. & Gibbons, J.F., *J. Appl. Phys.*, **5** (1984), 274.

8. Guenot, R. & Racinet, J., *British Welding Journal*, **14** (1967), 427.

9. Sekhar, J.A., Kou, S. & Mehrabian, R., *Metall. Trans.*, **14A** (1983), 1169.

10. Sekhar, J.A., Mehrabian, R. & Fraser, H.L., Proceedings of AIME Conference on Lasers in Metallurgy, 1982, p. 207.

11. Sekhar, J.A. & Mehrabian, R., *Metall. Trans.*, **12B** (1981), 411.

12. Brown, J.M. & Sekhar, J.A., *Metall. Trans.*, **15A** (1984), 29.

13. Sekhar, J.A., Proceedings of the Symposium on Amorphous Materials, Bhabha Atomic Research Centre, Bombay, October, 1983, p. 19.

14. Hode, J.M. & Joly, J.P., *Journal DC Physique*, October (1983), C5-343.

15. Grill, Shanir A. & Pelleg, J., *Metall. Trans.*, **118B** (1980). 257.

16. Kou, S., *Metall. Trans.*, **12A** (1981), 2025.

17. Kou, S., *Metall. Trans.*, **13A** (1982), 363.

18. Rama Rao, K.V. & Sekhar, J.A., *Acta Metall*, **15** (1986), 81.

19. Rama Rao, K.V. & Sekhar, J.A., *Metall. Trans.*, **18A** (1987), 354.